FACULDADE DE MEDICINA DA UNIVERSIDADE DE COIMBRA

TRABALHO FINAL DO 6º ANO MÉDICO COM VISTA À ATRIBUIÇÃO DO GRAU DE MESTRE NO ÂMBITO DO CICLO DE ESTUDOS DE MESTRADO INTEGRADO EM MEDICINA

RUI PEDRO RODRIGUES PEREIRA LEITÃO

HUNTINGTON'S DISEASE: MORPHOMETRIC CHANGES IN PRODROMAL AND DIAGNOSED PATIENTS

ARTIGO CIENTÍFICO

ÁREA CIENTÍFICA DE NEUROCIÊNCIAS

TRABALHO REALIZADO SOB A ORIENTAÇÃO DE:
DOUTORA GINA CAETANO
PROFESSOR MIGUEL CASTELO-BRANCO

ABRIL DE 2013

HUNTINGTON'S DISEASE: MORPHOMETRIC CHANGES IN PRODROMAL AND DIAGNOSED PATIENTS

Rui Pedro Rodrigues Pereira Leitão [(1)]

[(1)] FMUC – Faculty of Medicine, University of Coimbra, Portugal

Correspondence:

Rui Pedro Rodrigues Pereira Leitão

Mestrado Integrado em Medicina- 6º ano

Faculdade de Medicina da Universidade de Coimbra

Address: Rua das Fontainhas, 149, 3465-057 – Campo de Besteiros, Portugal

Email: ruipedroleitao@hotmail.com

ABSTRACT

Neuroimaging studies have proven to be a valuable resource in Huntington's disease (HD). As an autosomal dominant genetic disorder, it is possible to identify individuals before they manifest clinical symptoms ("prodromal HD"). This study was designed to assess if neuroimaging measures could be useful to successfully distinguish prodromal individuals from previously clinically diagnosed patients.

Seven participants with previously clinically diagnosed disease and eight individuals in a presymptomatic state underwent brain magnetic resonance imaging (MRI) and were matched and compared to a group of thirteen healthy controls. Cortical reconstruction and volumetric segmentation was performed with FreeSurfer 5.1.

We have found significant statistical differences on Caudate, Putamen and Globus Pallidus, from both hemispheres. Diagnosed group had smaller volumes when compared to Prodromal and Control group. Thickness maps derived from Diagnosed and Control groups' comparison revealed a thinning pattern affecting mostly the posterior and superior cerebral regions.

Our results suggest that structural MRI volumes and thickness maps can be useful to monitor Huntington's disease progression, allowing researchers to identify individuals in different stages of the disease. Clinical trials might benefit the most, by synergizing the current clinical diagnostic method with MRI measures to track neurodegenerative patterns of HD.

- **KEYWORDS**

Huntington's disease, MRI, cerebral cortex, cortical thickness, cross sectional analysis

INTRODUCTION

Huntington's disease (HD) is an autosomal dominant genetic, progressive, neurodegenerative disorder. The known genetic mutation has been identified as a CAG triplet repeat expansion in huntingtin (HTT) gene [1]. Longer CAG repeats imply an earlier onset, accounting for 50-70% of variance in age of onset. Repeat CAG lengths of 40 or more are associated with nearly full penetrance by age 65 years [2-4].

Worldwide, the prevalence of HD can go up to 10 per 100.000, but a recent meta-analysis by Pringsheim et al.[5] reported HD's prevalence to be 5.70 per 100.000 in the western world. The clinical diagnosis of HD is currently defined by "unequivocal presence of an otherwise unexplained extrapyramidal movement disorder". Chorea is the movement disorder typically associated with the disease, but bradykinesia, dystonia and rigidity will also affect the patient and are generally more disabling[6]. Besides these motor abnormalities, other clinical features of HD include cognitive decline (bradyphrenia, poor spatial and working memory, poor planning and organization, lack of judgment and poor mental flexibility) and psychiatric disturbances (depression, anxiety, disinhibition, aggressive behavior and a tendency to suicide). These criteria are subjective and highly-dependent on the raters' judgment of the severity of motor signs necessary to warrant a diagnosis.

There's no known cure for HD. Patients are managed by a multidisciplinary team, with regular support and symptomatic therapies. Most of therapies commonly used have not been addressed in clinical trials and its efficacy is not properly validated [6]. Researchers are trying to find biomarkers that would define disease states before a clinical diagnosis [7] .Therefore, the success of all efforts to find a solution for this problem depends on the development and validation of objective, quantifiable and feasible outcome measures to be used in clinical trials [8, 9].

Neuroimaging has gained increased attention in the last years, since it was established that

cognitive, sensory and psychiatric abnormalities precede motor symptoms in HD[10]. Predict-HD study results suggest that there might be detectable abnormalities from different markers (motor examination scores, odour recognition, striatal volumes and a wide range of cognitive performances) beginning 15 to 20 years prior the diagnosis of HD[11].

Previous neuroimaging studies indicate that significant brain atrophy occurs many years before the diagnosis of HD [7, 11-15]. So far, findings have included cerebral spinal fluids, regional cortical degeneration, striatal volumes, thalamus, abnormal thinning of cortical sulci, whole-brain atrophy, white matter and gray matter loss in subjects with early or pre-HD, suggesting that subtle morphological alterations in brain tissue are involved in natural course of HD and might be used as biomarkers for the disease. One of the most relevant structures is the striatum, with several studies reporting a volume loss greater than any other structure examined, making it a robust candidate as a biomarker for HD. Longitudinal studies suggest that there is a greater change over time in caudate than in putamen volume, but that there might be a stronger association between putamen and motor signs than between caudate and motor signs [13]. However, combining contributions from other areas (for example regional cortical atrophy, white matter atrophy) might provide a better solution than considering striatum volume contribution alone [13, 16].

Some studies have also demonstrated that oculomotor abnormalities are involved in early stages of HD and may be a potential candidate as a biomarker to monitor presymptomatic individuals. HD is characterized by saccade apraxia, with vertical saccades being affected more than horizontal saccades. Laboratory findings show increased saccade latency, marked variability in saccade latency and saccade slowing. We can also find increased directional errors and timing errors affecting antisaccades and memory-guided saccades. The extent of these changes correlates with disease severity [17].

The purpose of this study was to make a cross-sectional analysis of volume and thickness in order to determine whether neuroimaging measures could be useful in distinguishing successfully

individuals prospectively diagnosed with HD from individuals in a pre-symptomatic phase of HD and thus enhance the battery of outcome measures that could be used in clinical trials.

MATERIAL AND METHODS

- **Participants / Motor Function**

The results presented here are based on a sample of 28 individuals, from an ongoing longitudinal observational study conducted at Instituto Biomédico de Investigação de Luz e Imagem, Faculdade de Medicina da Universidade de Coimbra. All aspects of the study were approved by Local Ethics Committee, and all aspects of the study are in compliance with national legislation and the code of Ethics of the World Medical Association Declaration of Helsinki. All participants signed a written informed consent.

Participants with diagnosed disease were included in "HD" group, those in a prodromal phase in the "HP" group and healthy individuals in "HC" group. The sample included 15 individuals who tested positive for the HD gene mutation (CAG repeat lengths ranging from 40 to 48). Seven of these have been already diagnosed with the motor signs of HD at the time of study enrollment. Eight of these have been considered to be in the prodromal phase of disease according to the diagnostic confidence level of the Unified Huntington Disease Rating Scale UHDRS (scores of ≤5 would be classified as HP, scores >5 would be classified as HD if Total Functional Capacity scale was 10-13 and the Montreal Cognitive Assessment revealed no cognitive decline). Healthy control subjects were individually matched for age and gender to HP and HD group. Control subjects were excluded if they had an ophthalmologic disease, history of psychotropic drugs, history of neurologic or psychiatric illness, history of alcohol or drug abuse. All controls were also screened with Montreal Cognitive Assessment.

Table 1 provides demographic information on the three groups. HC group consisted of 6 men and 7 women, with an average age of 34.62 years (SD=9.39), who had an average of 11 years of education (SD=2.31). HP group consisted of 3 men and 5 women, with an average age of 34 years (SD=9.15), who had an average of 11.13 years of education (SD=3.8). HD group consisted of 3 men and 4 women, with an average age of 42 years (SD=7.19), who had an average of 10.71 years of education (SD=4.79).

Table 1. Demographics of Subjects

	HC	HP	HD
Age (years)	34.62 (9.39)	34.00 (9.15)	42.00 (7.19)
	22 - 55	19 - 48	35 - 57
Education (years)	11.00 (2.31)	11.13 (3.80)	10.71 (4.79)
	7 - 16	6 - 19	6 - 17
Male/Female	6 / 7	3 / 5	3 / 4
CAG (no. Repetitions)	NA	42 (2.16)	44.43 (2.30)
	NA	40 - 45	42 - 48

HC - Control subject group
HP - Prodromal disease group
HD - Diagnosed group

- **MRI Measures**

All participants underwent structural MRI scans using a 3T Siemens Magnetom Trio scanner (Erlangen, Germany), using a multi-echo MPRAGE sequence: 176 slices, acquisition times=6:03, voxel size=1x1x1 mm voxels, TR=2530, TE=1,64/3.5/6.36/7.22, FOV= 256mm (256x256 matrix), thickness=1 mm, 0 gap, NEX=2, flip angle=7, bandwidth 651 Hx/px for all echoes (bipolar readout

trajectory).

Cortical reconstruction and volumetric segmentation was performed with the software package FreeSurfer 5.1 (http://surfer.mmr.mgh.harvard.edu/).

Citing an adapted description of FreeSurfer methods, available on "http://surfer.nmr.mgh.harvard.edu/fswiki/FreeSurferMethodsCitation": "*Briefly, this processing includes motion correction and averaging (Reuter et al. 2010) of multiple volumetric T1 weighted images, removal of non-brain tissue using a hybrid watershed/surface deformation procedure (Segonne et al., 2004), automated Talairach transformation, segmentation of the subcortical white matter and deep gray matter volumetric structures (Fischl et al., 2002; Fischl et al., 2004a) intensity normalization (Sled et al., 1998), tessellation of the gray matter white matter boundary, automated topology correction (Fischl et al., 2001; Segonne et al., 2007), and surface deformation following intensity gradients to optimally place the gray/white and gray/cerebrospinal fluid borders at the location where the greatest shift in intensity defines the transition to the other tissue class (Dale et al., 1999; Dale and Sereno, 1993; Fischl and Dale, 2000). Once the cortical models are complete, a number of deformable procedures can be performed for in further data processing and analysis including surface inflation (Fischl et al., 1999a), registration to a spherical atlas which utilizes individual cortical folding patterns to match cortical geometry across subjects (Fischl et al., 1999b), parcellation of the cerebral cortex into units based on gyral and sulcal structure (Desikan et al., 2006; Fischl et al., 2004b), and creation of a variety of surface based data including maps of curvature and sulcal depth. This method uses both intensity and continuity information from the entire three dimensional MR volume in segmentation and deformation procedures to produce representations of cortical thickness, calculated as the closest distance from the gray/white boundary to the gray/CSF boundary at each vertex on the tessellated surface (Fischl and Dale, 2000). The maps are created using spatial intensity gradients across tissue classes and are therefore not simply reliant on absolute signal*

intensity. The maps produced are not restricted to the voxel resolution of the original data thus are capable of detecting subvoxel differences between groups. Procedures for the measurement of cortical thickness have been validated against histological analysis (Rosas et al., 2002) and manual measurements (Kuperberg et al., 2003; Salat et al., 2004). Freesurfer morphometric procedures have been demonstrated to show good test-retest reliability across scanner manufacturers and across field strengths (Han et al., 2006; Reuter et al., 2012).”

- **Statistical Analysis**

Volumes - Estimates of the volumes for non-neocortical structures were extracted and normalized for differences in estimated total intracranial volumes (eTIV) [18].The procedure used was “Value = (Structure Volume/eITV)*1000”. We did not use the covariance method for normalization and regression models would not be possible to apply at this stage. A list of the structures volumes before the coarse normalization procedure is displayed on table 2.

Since our data failed to meet the assumptions of ANOVA (the homogeneity of variance was violated), we had a small sample number (n=13/8/7) and to minimize the effects of outliers, it has been decided to use nonparametric tests to find differences between our groups.

For continuous outcome variables, Kruskal-Wallis (K-W) nonparametric tests were conducted to examine group differences in MRI volumes, corrected for eTIV, based on diagnostic status (HP vs HD), having another group (HC) as Control Group. There are no post-hoc tests built into the K-W test, so it has been decided to run three Mann-Whitney (M-W) tests comparing each pair of mean ranks, with the significance level being adjusted with a Bonferroni Correction. A significance level of .05 is used for all hypotheses testing unless specified otherwise. All statistical analyses were carried out with Statistical Package for the Social Sciences software (SPSS, version 17.0).

Table 2. Mean Freesurfer output volume values (cc)

	HC (n=13)	HP (n=8)	HD (n=7)
Left Caudate	3.86 (0.44)	3.08 (0.23)	2.29 (0.58)
Left Putamen	5.89 (0.84)	4.95 (0.69)	3.37 (0.82)
Left Globus Pallidus	1.86 (0.18)	1.58 (0.23)	1.05 (0.26)
Left Hippocampus	4.24 (0.39)	3.86 (0.27)	3.65 (0.49)
Left Amygdala	1.72 (0.18)	1.57 (0.24)	1.44 (0.16)
Left Accumbens	0.65 (0.11)	0.56 (0.13)	0.41 (0.12)
Right Caudate	3.93 (0.32)	3.23 (0.23)	2.43 (0.61)
Right Putamen	5.56 (0.66)	4.65 (0.60)	3.29 (0.72)
Right Globus Pallidus	1.52 (0.12)	1.37 (0.22)	0.99 (0.26)
Right Hippocampus	4.39 (0.33)	4.00 (0.22)	3.78 (0.51)
Right Amygdala	1.70 (0.14)	1.57 (0.22)	1.43 (0.24)
Right Accumbens	0.68 (0.11)	0.61 (0.11)	0.46 (0.15)
Cortical White Matter	517.3 (50.9)	457.70 (39.31)	465.69 (49.49)
Total Gray Matter	648.9 (54.2)	583.82 (41.92)	548.49 (53.22)

HC - Control subject group
HP - Prodromal disease group
HD - Diagnosed group
cc - cubic centimeters

Thickness maps were obtained with QDEC, an application included in the Freesurfer distribution. It was designed to aid researchers in performing inter-subject/group-averaging and inference on the morphometric data produced by the FreeSurfer processing stream (part of Freesurfer software package). In our General Linear Model, we applied a Gaussian smoothing with a FWHM=15mm and a Different Offset, Different Slope (DODS) design matrix type. Our statistical tests were corrected for multiple corrections using a false discovering rate (FDR) of 0.01. The cortical sulci and gyri labeling was based on Destrieux Atlas [19].

RESULTS

- **Volumetric Analysis**

Mean brain tissue volumes for each group (HC, HP, HD) as well as analyses of structure ratios (volumes divided by eTIV) are shown in table 3. General measures of Hippocampus, Amygdala and Cortical White Matter did not differ between groups. The structures that met our criteria for statistical significance were: Left Caudate, Left Putamen, Left Globus Pallidus, Left Accumbens, Right Caudate, Right Putamen, Right Globus Pallidus, Right Accumbens and Total Gray matter. Our post-hoc comparisons (using Mann-Whitney tests) are displayed on table 4, where we have found a statistical difference in these structures on Controls vs. HD and HP vs. HD. When comparing HD with controls, we have found smaller volumes on Caudate, Putamen, Globus Pallidus, from both hemispheres. Regarding HD vs. HP comparison, we have found differences on Left Caudate, Putamen, Globus Pallidus and Right Caudate and Putamen. We were not able to find any difference on structural volumes between HC and HP.

Table 3. Analysis of Regional Volumes				
	HC (n=13)	HP (n=8)	HD (n=7)	Statistic[a]
Structures	Volumes[b] (SD)			
Left Caudate	2.472 (0.250)	2.236 (0.205)	1.595 (0.399)	0.001
Left Putamen	3.766 (0.399)	3.612 (0.673)	2.353 (0.550)	0.001
Left Globus Pallidus	1.193 (0.095)	1.150 (0.167)	0.741 (0.195)	0.003
Left Hippocampus	2.716 (0.193)	2.796 (0.120)	2.567 (0.349)	0.357
Left Amygdala	1.106 (0.100)	1.139 (0.166)	1.012 (0.118)	0.175
Left Accumbens	0.419 (0.073)	0.408 (0.113)	0.288 (0.078)	0.027
Right Caudate	2.525 (0.205)	2.347 (0.222)	1.690 (0.402)	0.001
Right Putamen	3.557 (0.336)	3.396 (0.620)	2.308 (0.509)	0.001
Right Globus Pallidus	0.982 (0.089)	0.998 (0.185)	0.693 (0.186)	0.006
Right Hippocampus	2.813 (0.194)	2.904 (0.175)	2.663 (0.354)	0.283
Right Amygdala	1.091 (0.101)	1.136 (0.101)	1.000 (0.111)	0.079
Right Accumbens	0.433 (0.059)	0.445 (0.095)	0.321 (0.099)	0.036
Cortical White Matter	331.021 (21.555)	331.390 (18.317)	326.181 (17.844)	0.925
Total Gray Matter	415.396 (21.518)	423.482 (27.332)	384.611 (22.580)	0.027

HC - Control subject group

HP - Prodromal disease group

HD - Diagnosed group

[a] - p Value for Kruskal-Wallis test, based on eTIV-corrected volumes

[b] - Value = (Volume/eITV)*1000

Table 4. Analysis of Regional Volumes

	HC vs HP	HC vs HD	HP vs HD
Structures		Statistic[a]	
Left Caudate	0.104	< .0001	0.009
Left Putamen	0.75	< .0001	0.006
Left Globus Pallidus	0.75	< .0001	0.004
Left Accumbens	0.972	0.005	0.072
Right Caudate	0.104	< .0001	0.006
Right Putamen	0.595	< .0001	0.006
Right Globus Pallidus	0.645	0.001	0.014
Right Accumbens	0.972	0.011	0.054
Total Gray Matter	0.5	0.014	0.029

HC - Control subject group

HP - Prodromal disease group

HD - Diagnosed group

[a] - p Value for Mann-Whitney test, based on eTIV-corrected volumes

- **Thickness Maps**

We have only found statistical significant differences in the cortical thickness map derived from comparisons between HD and HC group (Figure 1) and in the map derived from HP and HC comparison (figure 2), on the left hemisphere. On table 5a, 5b and 6, there is a list of the most affected areas for each comparison, based on Destrieux Atlas. The coordinates shown are the standard QDEC output MNI305 coordinates. When comparing the cortical thickness between Controls and diagnosed subjects, we have found the most affected areas to be on occipital, superior temporal, superior frontal lobes and some parts of the parietal lobe. On the cortical thickness map that resulted from the comparison between Prodromal and Diagnosed group, we have only found significant differences on the left hemisphere, with the most affected regions being precuneus gyrus, circular sulcus of insula, temporal lobe, cingulate sulcus and occipital sulcus.

Figure 1 and 2 are corrected for multiple comparisons so that only statistically significant differences are displayed. Significance values are displayed as *–log(x)p* values. Minimum and maximum values of vertex p-values were 2.754 and 6.791 for left hemisphere, and 3.139 and 5.389 for right hemisphere, respectively. There were no significant differences in cortical thickness between other groups. Thinning is observed throughout most of the cerebral cortex, with the most affected regions being the occipital, temporal and frontal lobes.

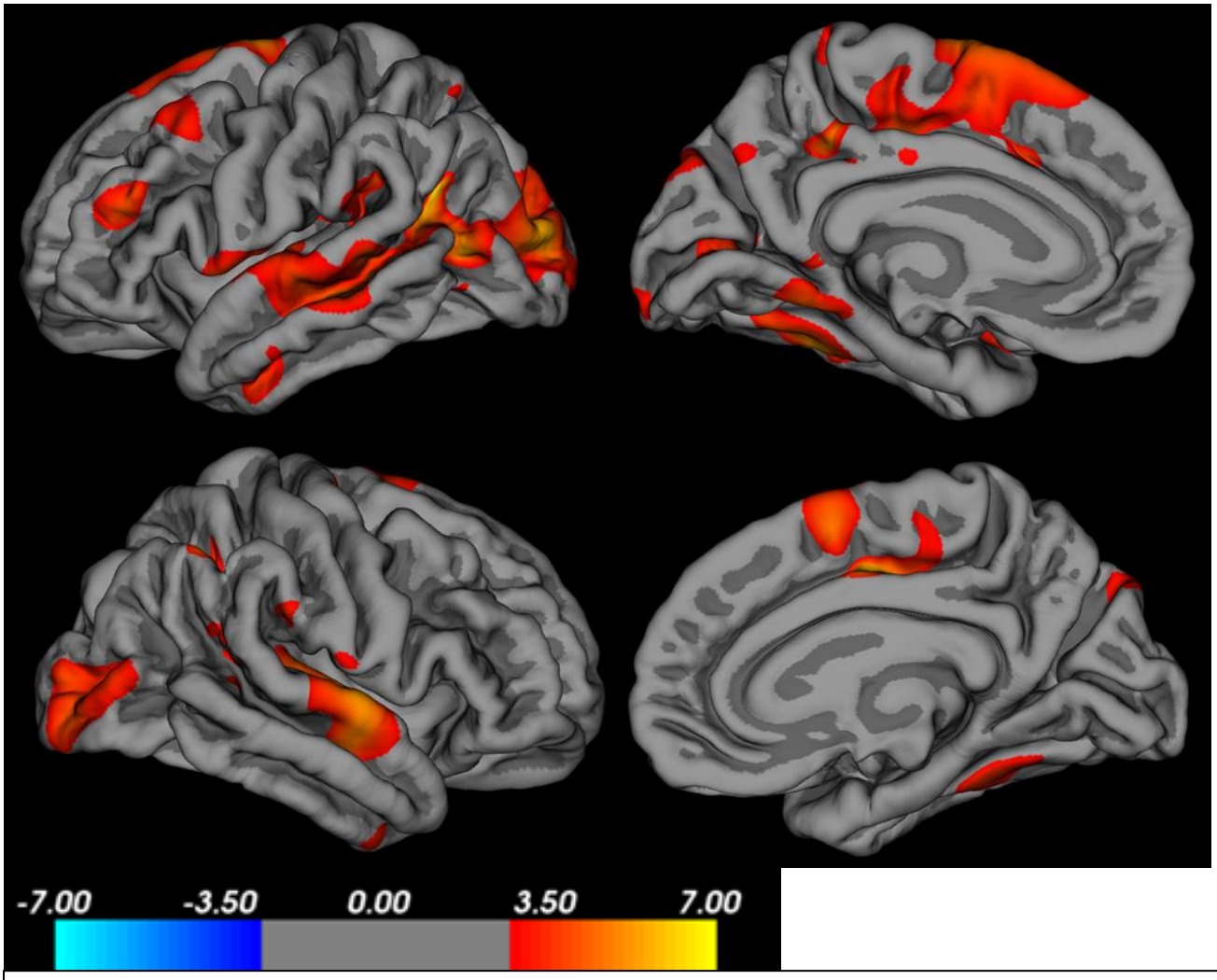

Figure 1 - Cortical Thickness Maps. First row is the left hemisphere; second row is the right hemisphere. Comparison of cortical thickness between HC (Controls) and HD (Diagnosed)

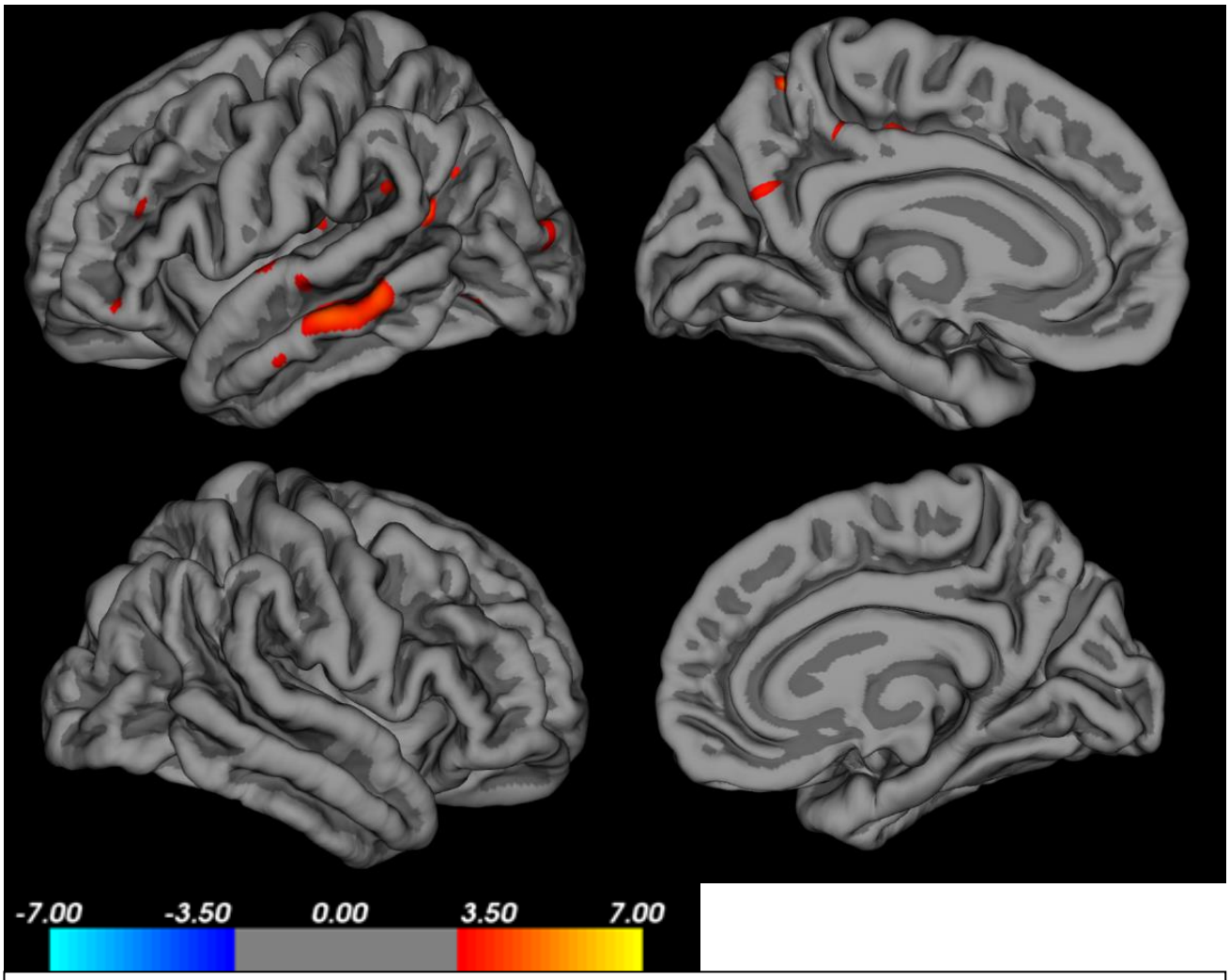

Figure 2 - Cortical Thickness Maps. First row is the left hemisphere; second row is the right hemisphere. Comparison of cortical thickness between HP (Prodromals) and HD (Diagnosed)

Table 5a. Analysis of Regional Thickness comparing HD to Controls		
Left Hemisphere		QDEC Coordinates
Region	pValue[a]	
S. Occipital superior and transversal	6.79	0.25, -89.11, 11.15
S. Temporal superior	6.37	-24.28, -64.60, 8.44
S. Circular insula superior	5.93	-19.77, 14.51, -8.47
G. Occipital middle	5.73	1.25, -101.98, -9.67
S. Occipital anterior	5.59	-23.65, -75.03, -16.63
G. Frontal superior	5.46	22.29, 23.38, 66.32
S. Temporal superior	5.39	-41.48, -15.62, -36.57
G. Occipitaltemporal lateral fusiform	5.35	-11.30, -36.69, -54.30
G. Temporal superior and transversal	5.12	-27.74, 4.56, -23.83
S. Subparietal	4.95	29.37, -35.08, 34.00
G. Frontal inferior opercular	4.61	-25.67, 33.19, -8.66
G. Occipitaltemporal medial lingual	4.3	13.57, -46.32, -35.02
S. Cingulate marginalis	4.18	28.56, -11.57, 40.24
S. Frontal superior	4.16	-2.69, 61-17, 35.98
G. and S. cingular mid post	4.14	29.19, 1.92, 43.43
S. Frontal inferior	4.12	-15.42, 67.95, 2.11
S. Circular insula inferior	3.99	-19.40, 28.04, -41.62
S. Calcarine	3.96	23.17, -71.83, -13.92
S. Circular insula superior	3.75	-12.97, 51.84, -22.70
S. Precentral (superior part)	3.68	-7.39, 14.24, 53.55
G. Temporal middle	3.66	-26.01, 15.96, -69.18

HD - Diagnosed group
S. - Sulcus, G. - Gyrus
[a] FDR - 0.01

Table 5b. Analysis of Regional Thickness comparing HD to Controls		
Right Hemisphere		QDEC Coordinates
Region	pValue[a]	
G. Angular (Parietal inferior lobule)	6.83	20.38, -44.95, 33.99
G. and S. Cingulate middle-posterior	6.17	-32.42, 23.72, 33.04
S. Intraparietal	5.68	4.19, -75.74, 24.81
G. Temporal superior lateral	5.49	33.10, 7.30, -29.68
G. Temporal superior and transversal	5.25	28.83, 6.70, -25.69
S. Temporal superior	5.02	36.17, 12.49, -41.08
G. Frontal superior	4.87	-29.54, 35.35, 54.81
S. Temporal transverse	4.6	31.20, -3.88, -16.06
Pole Occipital	4.42	2.55, -99.75, -27.41
G. Parietal inferior supramarginalis	4.02	38.58, -8.24, 14.90
S. Intraparietal	4.02	7.44, -45.28, 43.46
G. Occipitotemporal lateral fusiform	4.01	9.53, -33.20, -54.66
S. Temporal Superior	3.67	35.89, -35.60, -6.91
G. Occipital superior	3.51	-22.79, -84.80, 22.40

HD - Diagnosed group

S. - Sulcus, G. - Gyrus

[a] FDR - 0.01

Table 6. Analysis of Regional Thickness comparing HD to HP		
Regions of Left Hemisphere	pValue[a]	QDEC Coordinates
G. Precuneus	5.18	25.46, -57.28, 55.37
S. Circular insula superior	4.35	-18.61, 14.11, -9.08
S. Temporal superior	4.35	-28.88, -56.86, 2.25
G. Temporal middle	4.39	-41.07, -12.73, -46.14
S. Cingulate marginalis	4.3	28.37, -28.92, 40.44
S. Occipital superior and transversal	4.1	0.52, -90.68, 9.29
G. Temporal superior and transversal	3.95	-29.16, 7.74, -28.17
G. and S. Cingulate middle-posterior	3.82	28.86, -3.56, 44.69
S. Postcentral	3.81	-17.25, -27.36, 42.08

HP - Prodromal disease group
HD - Diagnosed group
S. - Sulcus, G. - Gyrus
[a] FDR - 0.01

DISCUSSION

Our findings confirm that volumetric and cortical thickness MRI measures can be used to successfully distinguish individuals prospectively diagnosed with HD from individuals in a pre-symptomatic phase of HD.

The hallmark of HD neuropathology is neurodegeneration in the caudate and putamen. It is accepted that striatal atrophy in clinical HD correlates with disease severity [20, 21]. Tabrizi, on a 24 month longitudinal study, demonstrated a close association between the progression of regional and whole-brain atrophy and clinical progression [15]. Furthermore, Aylward used caudate and putamen volumes to predict conversion from preclinical to clinical HD within 1 to 4 years, suggesting that atrophy in the preclinical phase implies significant ongoing neurodegeneration by the time a clinical diagnosis is made [13]. The results found here are in line with several studies regarding striatal volume in presymptomatic and diagnosed patients [22], showing that caudate and putamen are smaller in volume, when compared with control subjects. We have also included other structures in our analysis, with globus pallidus being the only one found to be reduced in volume in both HD and HP groups. Our initial statistical approach seemed to suggest that nucleus accumbens also revealed differences among the groups, but it did not survive a stricter post-hoc analysis.

Regarding the volumes of cerebral white matter and total gray matter, we have not found any difference between the groups. In a longitudinal analysis of brain morphology in prodromal HD subjects from PREDICT-HD study, it was reported that white-matter volumes significantly start decreasing far from onset, being most prominent in the frontal lobes [23]. Other authors also reported a significant white matter volume reduction in prodromal HD and early diagnosed HD patients [12, 14, 15, 24]. We were not able to confirm these results, with our analysis being focused on the whole cortical white matter volumes, whilst those studies have looked upon regional patterns of white matter

loss.

We also found differences in thickness measures between HD and HC, partially confirming the findings of previous neuroimaging results. As seen on figure 1, we have substantial thinning in the posterior cerebrum (occipital lobe), superior temporal, superior frontal, some areas of the parietal lobe. Nopoulos and Rosas used MRI to examine cortical thickness in clinical HD, finding widespread but heterogenous cortical thinning. It has been demonstrated that neurodegeneration of the cortex in HD occurs in a topographically, predictable, selective and progressive manner, with early affection of primary motor and visual cortices and that, in later stages, extended to pre-motor, anterior frontal, parieto-occipital, superior temporal and entorhinal cortices [14, 24, 25]. In our cross-sectional study, we have been able to assess this postero-anterior thinning pattern, but a longitudinal analysis is needed to confirm this data. In previous studies, Nopoulos reported finding differences between prodromal subjects and controls, but only on those near or mid onset, with a pattern in which the cortex was enlarged in the area of gyri , although it did not survive a stricter analysis, and substantially thinner cortex in the sulci[24]. Although we have found small differences on the left hemisphere when comparing the prodromal group with the diagnosed group, we were not able to find changes in cortical thickness on prodromal individuals when compared to controls. This may be caused by the heterogeneity of our group, as we did not separate our HP individuals according to predicted onset of disease because of small sample size. We also did not find any increase in the thickness of any cerebrum area, despite the fact that other studies [14, 24] found an increase of the rostral anterior cingulate in HP near onset and diagnosed groups. However, Nopoulos states that it might be due to a methodological bias.

Limitations of this study are mostly due to a small sample size. We were not able to sort our prodromal group according to the predicted years to diagnosis. The heterogeneity of our HP group might have masked differences versus controls, since it's established that far away individuals have

different findings from those near diagnosis. On our volumetric analysis, the use of parametric tests, as well calculations for effect size of our differences, was limited, as our data failed to meet the assumptions needed for this analysis [26, 27].

Despite these limitations, the data provided here is very promising. Our cross-sectional analysis allow us to confirm that there are morphometric changes on different stages of disease, giving the possibility to monitor the disease progression before a decline in cognitive or quantitative motor function is observed. We believe that with more subjects and a longitudinal analysis, it will be possible to have a more detailed and objective report regarding this data. Correlation between volume measures, thickness maps, oculomotor abnormalities and clinical symptoms will be assessed and reported. Thus, we expect to contribute with a better and broader analysis of the neuropathological pattern during Huntington's disease progression, corroborating some of the findings reported by other groups and, eventually, adding new data to the research.

Neuroimaging studies might be the way to provide clinical trials with new biomarkers to set up new clinical endpoints, in order to find pathological changes before overt motor symptoms and track disease progression [9, 10, 22, 28, 29]. Biomarker is "a characteristic that is objectively measured and evaluated as an indicator of normal biological processes, pathogenic processes or pharmacologic responses to a therapeutic intervention" [30]. We think that MRI methods such as structures volume and regional brain thickness are objective, reproducible and noninvasive, making them an excellent candidate, along with the early detection of these changes (up to 15 years before clinical diagnosis), the linear volume decline over time and the correlation with age at onset, length of nucleotide repeats. Further work is needed to find the precise relationship between these changes and clinical symptoms, but with large longitudinal studies coming to an end, we believe that morphometric markers may become a method to assess the effectiveness of a drug in clinical trials and, at the same time, be included in a screening battery to monitor the rate of progression of pathological changes in

presymptomatic individuals.

Our results suggest that structural MRI volumes and thickness maps can be useful to monitor Huntington's disease progression. Therapeutic trials should consider using MRI measures as an alternative or in addition to onset diagnosable outcome measures. However, it should not be used to clinically monitor patients in risk of developing motor signs. Not until there is a full predictive validity of these methods, physicians should not expect to use MRI measures to predict when diagnosable symptoms will occur.

Acknowledgements

This work was supported by the Portuguese Foundation for Science and Technology (PTDC/SAU-ENB/112306/2009). I thank Dr. Gina Caetano for all the support, Professor Miguel Castelo-Branco and study participants.

REFERENCES

1. MacDonald ME, Ambrose CM, Duyao MP, Myers RH, Lin C, Srinidhi L, et al. A novel gene containing a trinucleotide repeat that is expanded and unstable on Huntington's disease chromosomes. Cell. 1993;72(6):971-83.

2. Langbehn DR, Brinkman RR, Falush D, Paulsen JS, Hayden MR. A new model for prediction of the age of onset and penetrance for Huntington's disease based on CAG length. Clinical genetics. 2004;65(4):267-77. Epub 2004/03/18.

3. Aylward E, Mills J, Liu D, Nopoulos P, Ross CA, Pierson R, et al. Association between Age and Striatal Volume Stratified by CAG Repeat Length in Prodromal Huntington Disease. PLoS currents. 2011;3:RRN1235. Epub 2011/05/20.

4. Langbehn DR, Hayden MR, Paulsen JS. CAG-repeat length and the age of onset in Huntington disease (HD): a review and validation study of statistical approaches. American journal of medical genetics Part B, Neuropsychiatric genetics : the official publication of the International Society of Psychiatric Genetics. 2010;153B(2):397-408. Epub 2009/06/24.

5. Pringsheim T, Wiltshire K, Day L, Dykeman J, Steeves T, Jette N. The incidence and prevalence of Huntington's disease: a systematic review and meta-analysis. Movement disorders : official journal of the Movement Disorder Society. 2012;27(9):1083-91. Epub 2012/06/14.

6. Phillips W, Shannon KM, Barker RA. The current clinical management of Huntington's disease. Movement disorders : official journal of the Movement Disorder Society. 2008;23(11):1491-504. Epub 2008/06/27.

7. Soneson C, Fontes M, Zhou Y, Denisov V, Paulsen JS, Kirik D, et al. Early changes in the hypothalamic region in prodromal Huntington disease revealed by MRI analysis. Neurobiology of disease. 2010;40(3):531-43. Epub 2010/08/05.

8. Paulsen JS, Long JD. Neurodegenerative disease: Establishing a clinical trial battery for Huntington disease. Nature reviews Neurology. 2012;8(5):250-1. Epub 2012/04/11.

9. Ross CA, Tabrizi SJ. Huntington's disease: from molecular pathogenesis to clinical treatment. Lancet neurology. 2011;10(1):83-98. Epub 2010/12/18.

10. Paulsen JS. Functional imaging in Huntington's disease. Experimental neurology. 2009;216(2):272-7. Epub 2009/01/28.

11. Paulsen JS, Langbehn DR, Stout JC, Aylward E, Ross CA, Nance M, et al. Detection of Huntington's disease decades before diagnosis: the Predict-HD study. Journal of Neurology, Neurosurgery & Psychiatry. 2008;79(8):874-80.

12. Paulsen JS, Nopoulos PC, Aylward E, Ross CA, Johnson H, Magnotta VA, et al. Striatal and white matter predictors of estimated diagnosis for Huntington disease. Brain research bulletin. 2010;82(3-4):201-7. Epub 2010/04/14.

13. Aylward EH, Liu D, Nopoulos PC, Ross CA, Pierson RK, Mills JA, et al. Striatal volume contributes to the prediction of onset of Huntington disease in incident cases. Biological psychiatry. 2012;71(9):822-8. Epub 2011/09/13.

14. Rosas HD, Salat DH, Lee SY, Zaleta AK, Pappu V, Fischl B, et al. Cerebral cortex and the clinical expression of Huntington's disease: complexity and heterogeneity. Brain : a journal of neurology. 2008;131(Pt 4):1057-68. Epub 2008/03/14.

15. Tabrizi SJ, Reilmann R, Roos RA, Durr A, Leavitt B, Owen G, et al. Potential endpoints for clinical trials in premanifest and early Huntington's disease in the TRACK-HD study: analysis of 24 month observational data. Lancet neurology. 2012;11(1):42-53. Epub 2011/12/06.

16. Paulsen JS, Magnotta VA, Mikos AE, Paulson HL, Penziner E, Andreasen NC, et al. Brain structure in preclinical Huntington's disease. Biological psychiatry. 2006;59(1):57-63. Epub 2005/08/23.

17. Tim JA, Michael RM. Eye movements in patients with neurodegenerative disorders. Nature Reviews Neurology. 2013;9(2):74-85.

18. Buckner RL, Head D, Parker J, Fotenos AF, Marcus D, Morris JC, et al. A unified approach for morphometric and functional data analysis in young, old, and demented adults using automated atlas-based head size normalization: reliability and validation against manual measurement of total intracranial volume. NeuroImage. 2004;23(2):724-38. Epub 2004/10/19.

19. Fischl B, van der Kouwe A, Destrieux C, Halgren E, Segonne F, Salat DH, et al. Automatically parcellating the human cerebral cortex. Cereb Cortex. 2004;14(1):11-22. Epub 2003/12/05.

20. Kassubek J, Juengling FD, Ecker D, Landwehrmeyer GB. Thalamic atrophy in Huntington's disease co-varies with cognitive performance: a morphometric MRI analysis. Cereb Cortex. 2005;15(6):846-53. Epub 2004/10/02.

21. Aylward EH. Change in MRI striatal volumes as a biomarker in preclinical Huntington's disease. Brain research bulletin. 2007;72(2-3):152-8. Epub 2007/03/14.

22. Bohanna I, Georgiou-Karistianis N, Hannan AJ, Egan GF. Magnetic resonance imaging as an approach towards identifying neuropathological biomarkers for Huntington's disease. Brain research reviews. 2008;58(1):209-25. Epub 2008/05/20.

23. Aylward EH, Nopoulos PC, Ross CA, Langbehn DR, Pierson RK, Mills JA, et al. Longitudinal change in regional brain volumes in prodromal Huntington disease. Journal of Neurology, Neurosurgery & Psychiatry. 2011;82(4):405-10.

24. Nopoulos PC, Aylward EH, Ross CA, Johnson HJ, Magnotta VA, Juhl AR, et al. Cerebral cortex structure in prodromal Huntington disease. Neurobiology of disease. 2010;40(3):544-54. Epub 2010/08/07.

25. Nopoulos P, Magnotta VA, Mikos A, Paulson H, Andreasen NC, Paulsen JS. Morphology of the cerebral cortex in preclinical Huntington's disease. The American journal of psychiatry. 2007;164(9):1428-34. Epub 2007/08/31.

26. Morgan GA, Leech, N. L., Gloeckner, G. W., & Barrett, K. C. . SPSS for introductory statistics: Use and Interpretation. . Mahwah, NJ.: Lawrence Erlbaum Associates.; 2004.

27. Maroco JP. Análise Estatística com o PASW Statistics (ex-SPSS). Pêro Pinheiro: ReportNumber; 2010. 963 p.

28. Rosas HD, Feigin AS, Hersch SM. Using advances in neuroimaging to detect, understand, and monitor disease progression in Huntington's disease. NeuroRx : the journal of the American Society for Experimental NeuroTherapeutics. 2004;1(2):263-72. Epub 2005/02/18.

29. Paulsen JS. Early detection of Huntington's disease. Future Neurology. 2009;5(1):85-104.

30. Biomarkers and surrogate endpoints: preferred definitions and conceptual framework. Clinical pharmacology and therapeutics. 2001;69(3):89-95. Epub 2001/03/10.